Free Radical Biology & Medicine 46 (2009) 1362–1375

Contents lists available at ScienceDirect

Free Radical Biology & Medicine

journal homepage: www.elsevier.com/locate/freeradbiomed

Original Contribution

Inhibition of γ-secretase activity reduces Aβ production, reduces oxidative stress, increases mitochondrial activity and leads to reduced vulnerability to apoptosis: Implications for the treatment of Alzheimer's disease

Baiyang Sheng [a], Kai Gong [a], Ying Niu [a], Lingling Liu [a], Yufang Yan [a], Guangyuan Lu [a], Lihai Zhang [b], Min Hu [c], Nanming Zhao [a], Xiufang Zhang [a], Peifu Tang [b], Yandao Gong [a,b,*]

[a] State Key Laboratory of Biomembrane and Membrane Biotechnology, Department of Biological Sciences and Biotechnology, Tsinghua University, Beijing 100084, China
[b] Department of Orthopaedics, Chinese PLA General Hospital, Beijing 100853, China
[c] Department of Stomatology, Chinese PLA General Hospital, Beijing 100853, China

ARTICLE INFO

Article history:
Received 21 August 2008
Revised 24 January 2009
Accepted 18 February 2009
Available online 3 March 2009

Keywords:
Alzheimer's Disease
presenilins
γ-secretase
Oxidative stress
Mitochondria
Apoptosis

ABSTRACT

It has been argued that γ-secretase should be considered as a pharmacological target, as there are few mechanism-based experimental and clinical studies on γ-secretase treatment. In this study, we found that N2a cells bearing APP695 or its Swedish mutant exhibited increased basal levels of ROS, nitric oxide (NO), protein carbonyls, MDA and intracellular calcium, as well as reduced level of the mitochondrial membrane potential and ATP. When the activity of γ-secretase was inhibited by expression of the D385A PS1 variant, cells (N2a/Swe.D385A) showed reduced basal levels of ROS, nitric oxide (NO), protein carbonyls, MDA and intracellular calcium, as well as increased mitochondrial membrane potential and ATP level. In addition, N2a/Swe.D385A cells showed reduced vulnerability to H_2O_2-induced apoptosis. The Bcl-2 and JNK/ERK pathways were proven to be involved in the change of vulnerability to H_2O_2-induced apoptosis. Moreover, we discovered that inhibition of γ-secretase by DAPT would lead to a reduction of ROS levels and stabilization of mitochondrial function in APP (N2a/APP695) and APP Swedish mutant (N2a/APPswe) transfected cells. At last, it was shown that Aβ antibody and antiserum prevented increase of ROS and reduction of mitochondrial membrane potential in N2a/Swe.ΔE9 cells but not in N2a/Swe.D385A cells, which indicated that reduced formation of Aβ was the reason for reduction of ROS formation and increase of mitochondrial membrane potential when PS-1 activity was impaired in N2a/Swe.D385A cells. We concluded that neurotoxicity was positively correlated with the activity of γ-secretase, which suggested inhibition of γ-secretase is a rational pharmacological target for Alzheimer's disease treatment.

Introduction

Alzheimer's disease (AD), the most common progressive neurodegenerative disease, is pathologically characterized by senile plaques (SP), intracellular neurofibrillary tangles (NFT) and neuronal death [1-4]. The primary protein component of SP is β-amyloid peptide (Aβ), which is derived from the amyloid precursor protein (APP) through an initial cleavage by β-secretase followed by an intramembranous cut by γ-secretase. γ-secretase is a large multimeric membrane-bound protein composed of presenilins (PS1 and PS2), nicastrin, PEN-2 and Aph-1. Mutations in three different genes, APP and presenilin-1 and -2 (PS1 and PS2), are known to cause early onset familial AD (FAD) [5,6]. These mutations alter proteolytic processing of APP resulting in an overproduction and aggregation of neurotoxic forms of Aβ. Aβ is now widely considered to play a central role in the pathogenesis of AD, although it is not known whether this is direct [7,8] or indirect [9]. In any case, the mechanisms through which Aβ impairs neuronal function are still unknown.

Oxidative stress and mitochondrial dysfunction have been observed in the AD brain [10-12]. The reduced energy metabolism in AD may be due to oxidative dysfunction of some key metabolic or mitochondrial enzymes [13-15]. It was reported that APP/PS-1 double mutant neurons displayed a significant basal increase in reactive oxygen species (ROS) when compared with the wild-type neurons [16]. ROS is highly reactive with biomolecules, including proteins, lipids, carbohydrate, DNA and RNA, which have been well documented to increase in AD [17]. Furthermore, studies indicated that Aβ oligomers could impair mitochondrial function via ROS production and further increase ROS levels [18]. In addition to the direct effects, oxidative stress could also stimulate additional damage in the brain via the overexpression of inducible nitric oxide synthase (iNOS) and the action of constitutive neuronal NOS (nNOS) that increase the

* Corresponding author. Department of Biological Sciences and Biotechnology, Tsinghua University, Beijing 100084, China. Fax: +86 10 62794214.
E-mail addresses: pftang301@126.com (P. Tang), gongyd@tsinghua.edu.cn (Y. Gong).

0891-5849/$ – see front matter © 2009 Elsevier Inc. All rights reserved.
doi:10.1016/j.freeradbiomed.2009.02.018

production of nitric oxide ($NO^{\cdot}$) and its derivative (reactive nitrogen species) [19,20]. Mitochondrion is an important reserve pool of intracellular Ca^{2+}. This organelle works as a regulator of intracellular Ca^{2+} homeostasis. Conversely, impairment of mitochondrial function can result in increased cytoplasmic calcium levels. Increased mitochondrial Ca^{2+} overload has been associated with the release of proapoptotic mitochondrial proteins, leading to cell death. Studies of experimental models of AD suggested that mitochondrial impairment may promote dysregulation of neuronal calcium homeostasis [21].

Many oxidative stress factors have been shown to trigger apoptosis by stimulating stress-activated protein kinases (SAPKs) such as JNK and $p38^{MAPK}$ [22-24]. In AD model cells, it was shown that the APP Swedish mutation enhanced the vulnerability to oxidative stress, finally leading to apoptotic cell death through the activation of the c-Jun N-terminal kinase, caspases 3 and 9 [25] and a shift in the Bcl-xL/Bax ratio toward Bax [26]. A study indicated that Aβ-induced apoptosis not only required oxidative stress-mediated activation of SAPKs, but also operated through recruitment of classic apoptotic mitochondrial regulatory proteins, such as p53 and Bcl-2 [27].

As outlined above, it seems that a myriad of factors and signaling pathways are involved in the relationship of Aβ, oxidative stress and mitochondrial dysfunction. However, it is still not clear whether the oxidative stress is the cause or result of the process of Aβ plaque formation. Recent evidence has indicated that mitochondria serve as intracellular aggregation sites for Aβ. Although both monomers and oligomers of Aβ are present within mitochondria [28-30], the potential effects of Aβ on mitochondrial function are still an enigma.

More than 150 FAD-linked PS1 mutations have been identified to date and are suggested to affect γ-secretase activity to different extents. Several studies showed that expression of mutant PS1 or PS2 in cells led to enhanced generation of both intracellular [31] and extracellular [32] Aβ42, while there was an article [33] showing that presenilin clinical mutations could affect γ-secretase activity by different mechanisms and led to a relative increase in the ratio of the Aβ42 to Aβ40 peptides but did not increase Aβ42. Hence, γ-secretase has been considered as a plausible molecular target as a means to interfere with the production of Aβ. However, there has been little research on the correlative mechanism. A recent study indicated that moderate reduction of γ-secretase showed promise as a clinical therapy [34]. Expression of the PS1 harboring aspartate to alanine substitution at codon 385 (D385A) reduced the levels of secreted Aβ peptides in mouse neuroblastoma, N2a cells [35]. In this study, we investigated the negative effect on oxidative stress, mitochondrial function and Ca^{2+} homeostasis of endogenous Aβ overproduction by using N2a cell lines stably transfected with wild-type APP (N2a/APP695) or Swedish mutant APP (N2a/APPswe). We also tested the hypothesis that reduction in the level of secreted Aβ via inhibiting the activity of γ- secretase would decrease the negative effects on oxidative stress, mitochondrial function and Ca^{2+} homeostasis by using N2a cell lines stably co-transfected with Swedish mutant forms of APP genes and PS1 D385A mutant genes (N2a/Swe.D385A). And then we observed that N2a/Swe.D385A cells showed reduced vulnerability to a secondary insult, compared to cells expressing wild type PS1 (N2a/Swe.wt) or an FAD PS1ΔE9 mutation (N2a/Swe.ΔE9). At last, we proved that reduced formation of Aβ was the reason for reduction of ROS formation and increase of mitochondrial membrane potential when PS-1 activity was impaired in N2a/Swe.D385A cells.

Materials and methods

Materials

N-[N-(3,5-Difluorophenacetyl)-L-alanyl]-Sphenylglycinet-butyl ester (DAPT), antibody 4G8 against Aβ, butyric acid, 2,7-dichlorofluorescin-diacetole (DCFH-DA), Rhodamine 123, 3-(4,5-dimethylthiazol- 2-yl)-2,5-diphenyltetrazolium bromide (MTT), Hoechest33258 and propidium iodide (PI) were obtained from Sigma (St. Louis, MO, USA). Anti-dinitrophnol antibody was purchased from Zymed Antibody Inc., USA. LDH kit was obtained from promega, USA. NO indicator 3-Amino, 4-aminomethyl-2′, 7′-difluorescein, diacetate (DAF-FM DA) and ATP assay kit were purchased from Beyotime (Jiangsu, China). The assay kit for malondialdehyde (MDA) was purchased from Nanjing Jiancheng Bioengineering Institute (Nanjing, China). Calcium indicator Fluo3/AM was obtained from Calbiochem, USA. Antibodies against JNK, Erk, Bax, Bcl-2and Actin were obtained from Santa Cruz, USA.

Cell culture

Mouse neuroblastoma N2a cells and their derivative clones stably expressing human APP695 (N2a/APP695) or human Swedish mutation (K670M/N671L) APP695 (N2a/APPswe) gene, co-transfected with human APP695 harboring the “Swedish” double mutant and human wt PS1 or various PS1 mutants [36] were obtained from Dr. Huaxi Xu (The Burnham Institute, SD, USA). The cells were maintained in 50% Dulbecco's modified Eagle's medium (DMEM), 50% OPTI-MEM plus 5% fetal bovine serum in the presence of 200 μg/ml G418.

Measurement of intracellular ROS

To determine the intracellular ROS, N2a cells were plated at a density of 1×10^5 cells/ml the day before measurement. N2a cells were incubated with butyric acid (5 mM), DAPT (250 nM), H_2O_2 (50 μM), Aβ monoclonal antibody 4G8 (0.05%), or anti Aβ1-10 serum (0.05%) for different time. Cells were rinsed with Krebs' ringer solution (100 mM NaCl, 2.6 mM KCl, 25 mM $NaHCO_3$, 1.2 mM $MgSO_4$, 1.2 mM KH_2PO_4 and 11 mM glucose), and 10 μM DCFH-DA was loaded. After incubation at 37°C in a 5% CO_2 incubator for 1 h, cells were washed five times with the same buffer and examined under a confocal fluorescence microscope (FV500, Olympus) equipped with an argon laser. The digital images were analyzed with Image-Pro Plus software (ver 5.0). The average fluorescent density of intracellular areas was measured to index the ROS level.

Determination of the mitochondrial membrane potential (Ψ_m)

To determine the mitochondrial membrane potential (Ψ_m), N2a cells were plated the day before at a density of 1×10^5 cells/ml. N2a cells were incubated with butyric acid (5 mM), DAPT (250 nM), H_2O_2 (50 μM), Aβ monoclonal antibody 4G8 (0.05%), or anti Aβ1-10 serum (0.05%) for different time. Fluorescence dye Rhodamine 123 was added to the cell culture medium at a concentration of 1 μM for 15 min. And then the cells were washed five times with Krebs' ringer solution (100 mM NaCl, 2.6 mM KCl, 25 mM $NaHCO_3$, 1.2 mM $MgSO_4$, 1.2 mM KH_2PO_4 and 11 mM glucose) and examined under a confocal fluorescence microscope (FV500, Olympus) equipped with an argon laser. The digital images were analyzed with Image-Pro Plus software (ver 5.0). The average fluorescent density of intracellular areas was measured to index the Ψ_m level.

Protein carbonyl assay

Oxidative protein modification was estimated via measurement of protein carbonyl content by Elisa [37]. Basically, protein carbonyls were reacted with 2, 4-dinitrophenylhydrazine (DNPH) and the hydrazone adducts were detected with anti-DNP antibody. Oxidized BSA containing additional carbonyls was prepared for use as a reference by reacting (at 50 mg/ml in PBS) with hypochlorous acid (final concentration 5 mM) for 1 h at 37°C, followed by overnight dialysis against PBS at 4°C. For fully reduced BSA, a 0.01 g/ml natural BSA solution in PBS was used to react with 0.02 g/ml sodium

borohydride for 30 min, followed by neutralization with 2 M HCl and overnight dialysis against PBS. DNPH was combined with the BSA standards and the carbonyl content was determined colorimetrically by measuring the absorbance at 375 nm ($\varepsilon = 22{,}000\ M^{-1}\ cm^{-1}$) [38]. BSA standards were prepared by mixing various proportions of oxidized or reduced BSA, giving a final concentration of 4 mg protein/ml with a range of protein carbonyl contents. The concentration of protein samples of unknown carbonyl content was also adjusted to 4 mg protein/ml. The samples and standards were incubated with 3 volumes of 10 mM DNPH in 6 M guanidine-HCl and 0.5 M potassium phosphate (pH 2.5) for 45 min at room temperature with mixing every 10-15 min. 5 μl aliquots of each reaction mixture were mixed with 1 ml PBS and 200 μl replicates were added per well to 96-well immunoplates. The samples were incubated overnight at 4°C. After washing with PBS, nonspecific binding sites were blocked with 300 μl 0.1% reduced BSA in PBS for 2 h at 37°C. Wells were incubated with anti-DNP antibody (1:1,000 dilution in 0.1% Tween 20/PBS) for 1 h at 37°C, followed by incubation with a secondary rat anti-mouse monoclonal antibody, conjugated to horseradish peroxidase (1:3,000 dilution in 0.1% Tween 20/PBS). An o-phenylenediamine/peroxide solution (200 μl) was added to the reaction mixture for 5 min (terminated with 100 μl of 2.5 M sulfuric acid) and read at 490 nm. The specific absorbance for each sample was calculated by subtracting the basal absorbance of the DNP reagent from the total absorbance.

Intracellular NO detection

The intracellular NO level ($[NO]_i$) was measured using a NO-sensitive fluorescence probe DAF-FM DA by confocal microscopy as described previously [39]. Briefly, cells were loaded with DAF-FM DA (10 μM) at 37°C for 30 min in Krebs' ringer solution (100 mM NaCl, 2.6 mM KCl, 25 mM $NaHCO_3$, 1.2 mM $MgSO_4$, 1.2 mM KH_2PO_4 and 11 mM glucose). Then cells were gently washed three times and incubated for another 30 min to ensure complete cleavage of DAF-FM DA by the intracellular ester enzyme to release the NO-sensitive probe (DAF-FM). Fluorescence was detected with a laser scanning confocal microscope (FV 500, Olympus, Japan). The digital images were analyzed with Image-Pro Plus software (ver 5.0). The average fluorescent density of intracellular areas was measured to index the NO level.

MDA Determination

MDA, a compound that is produced during lipid peroxidation, was determined by thiobarbituric acid (TBA) test as described in [40]. MDA was reacted with thiobarbituric acid (TBA,) forming MDA-(TBA)2, a red-colored adduct with maximum absorbance at 532 nm. MDA in cell homogenate was measured and calculated according to manufacturer's protocol of MDA assay kit.

Determination of ATP Levels with a Bioluminescence Assay

The level of ATP in N2a cell lines was determined using the ATP Bioluminescence Assay Kit. Briefly, harvested cultured cells were lysed with a lysis buffer, followed by centrifugation at 10,000 ×g for 2 min at 4°C. Finally, the level of ATP was determined by mixing 50 μl of the supernatant with 50 μl of luciferase reagent, which catalyzed the light production from ATP and luciferin. The emitted light was linearly related to the ATP concentration and measured using a microplate luminometer.

Detection of intracellular calcium

The $[Ca^{2+}]_i$ in cells was measured using the indicator Fluo3/AM. Fluo3/AM was solubilized in DMSO. Briefly, cells were loaded with 5 μM Fluo3/AM in HBSS (145 mM NaCl, 2.5 mM KCl, 1 mM $MgCl_2$, 20 mM HEPES, 10 mM glucose and 1.8 mM $CaCl_2$) at 37°C for 30 min. After washed three times, cells were incubated for another 30 min to ensure complete cleavage of Fluo3/AM by intracellular ester enzyme to release calcium-sensitive probe (Fluo-3). The fluorescent dye was excited at 488 nm, and the changes in fluorescence were monitored using a confocal microscope (FV 500, Olympus, Japan).

LDH Determination

The release of lactate dehydrogenase (LDH) is a marker of cell membrane integrity. LDH release into the cultured medium was detected using a colorimetric reaction reading of absorbance at 490 nm according to manufacturer's protocol of LDH assay kit.

Cell viability

Cell viability was determined by the MTT reduction assay method. The N2a cells were cultured with different concentrations of H_2O_2 for 24 h in 96-well plates. MTT was added to each well with a final concentration of 1.0 mg/ml and the samples were incubated for 1 h in a CO_2 incubator. After 4 h incubation at 37°C, the MTT solution was removed and the insoluble formazane crystal was dissolved in DMSO. The absorbance at 570 nm was measured using a microplate reader.

Morphological analysis of apoptosis

To visualize the nuclear morphology and chromatin condensation with a confocal microscope, cells were incubated with H_2O_2 (50 μM) in an atmosphere with 5% CO_2 at 37°C for 24 h. Cells were stained with 50 μg/ml Hoechst 33258 and 50 μg/ml propidium iodide. The nuclear morphology and chromatin condensation were observed by confocal microscopy. Apoptotic cells showed blue nuclear condensation and fragmentation, while necrotic cells showed red fluorescence as stained by propidium iodide. The fractions of apoptotic and necrotic cells were determined relative to total cells. At least 200 cells were counted in each experiment.

Western blot

About 1×10^7 N2a cells were collected each time. Cell lysates were prepared in 500 μl RIPA buffer containing 50 mM Tris-HCl, pH 7.4, 150 mM NaCl, 0.5% Nonidet P-40 and 1 mM each of EDTA, EGTA, phenylmethyslysulfonyl fluoride and Na_3VO_4, and 10 μg/ml each of the protease inhibitors leupeptin, aprotinin and pepstatin followed by sonication for 10 s on ice. The lysates were then centrifuged at 10,000 rpm for 10 min at 4°C. The protein content of the supernatants was determined using the Bio-Rad protein assay reagent (bicinchoninic acid). Then the samples were mixed with 4 ×sodium dodecyl sulfate-polyacrylamide gel electrophoresis (SDS-PAGE) sample buffer (60 mM Tris, pH 6.8, 10% glycerol, 2% SDS, 10% β-mercaptoethanol and 0.005% bromophenol blue) and boiled for 5 min at 100°C. The supernatants used for immunoblotting proteins were separated by 10% SDS-PAGE and were electrotransferred onto nitrocellulose membrane (pore size 0.45 μm). Immunoblots were analyzed using specific primary antibodies against specific proteins. After incubation with alkaline phosphatase-conjugated secondary antibodies, proteins were visualized by development using Sigma fast tablets (BCIP/NBT substrate). The bands on the membrane were scanned and analyzed using the Pro-Plus imaging software (Ver 5.0).

Aβ measurement

The Aβ production of the supernatants was measured by trichloroacetic acid (TCA) precipitation [41] and Tris-Tricine SDS-PAGE. Briefly, culture medium without serum was collected, treated with protease inhibitors (1 μg/ml pepstatin, 10 μg/ml leupeptin and

1 mM phenylmethylsulfonyl fluoride) and BSA (0.1%). Supernatants were mixed with equal volumes of 20% TCA. After 30 min at 4°C, the samples were centrifuged at 18000 ×g for 15 min at 4°C. The supernatants were removed and the pellets were washed with ice-cold acetone. After centrifugation at 10000 ×g for 5 min at 4°C, the pellets were dried and dissolved with RIPA buffer containing 50 mM Tris-HCl, pH 7.4, 150 mM NaCl, 0.5% Nonidet P-40 and 1 mM each of EDTA, EGTA, phenylmethyslysulfonyl fluoride and Na_3VO_4. Then the Aβ content was assessed by Tris-Tricine SDS-PAGE as described previously [35,42].

Results

Basal levels of ROS, protein carbonyls, $[NO]_i$ and MDA were increased in N2a/APP695 and N2a/APPswe cells

The levels of NO, ROS, protein carbonyls and MDA are four essential parameters of oxidative stress [17]. Thus, we measured the intracellular NO, ROS, protein carbonyl and MDA levels in our cell models. N2a/APP695 and N2a/APPswe cells showed increased production of Aβ (Fig. 1a). To study the possible role of endogenous Aβ in regulating oxidative stress, we first compared the profile of intracellular ROS, protein carbonyls and $[NO]_i$ in N2a/APP695 cells and N2a/APPswe cells with wild-type N2a cells. The results indicated that the levels of ROS (Fig. 1b), protein carbonyls (Fig. 1c) and $[NO]_i$ (Fig. 1d) were significantly enhanced in the following order: control cells< N2a/APP695< N2a/APPswe. Oxidative stress arised in our transgenic cells was accompanied by increased lipid peroxides. As shown in Fig. 1e, intracellular malondialdehyde (MDA), a product of lipid peroxidation, was increased by 81% in N2a/APP695 and by 112% in N2a/APPswe cells ($P<0.005$ vs. control, respectively). Consistent with our results, previous studies have shown that intracellular ROS is elevated in APP/PS1 double mutant neurons [16]. Moreover, protein carbonyls were found to increase in vulnerable regions of the AD brain [43], AD model mice [44] and model cells [16].

Endogenous Aβ led to mitochondrial damage and increased $[Ca^{2+}]_i$

Ψ_m is a very important marker for the function of mitochondria. Aβ treatment of PC12 cells has been shown to lead to a significant

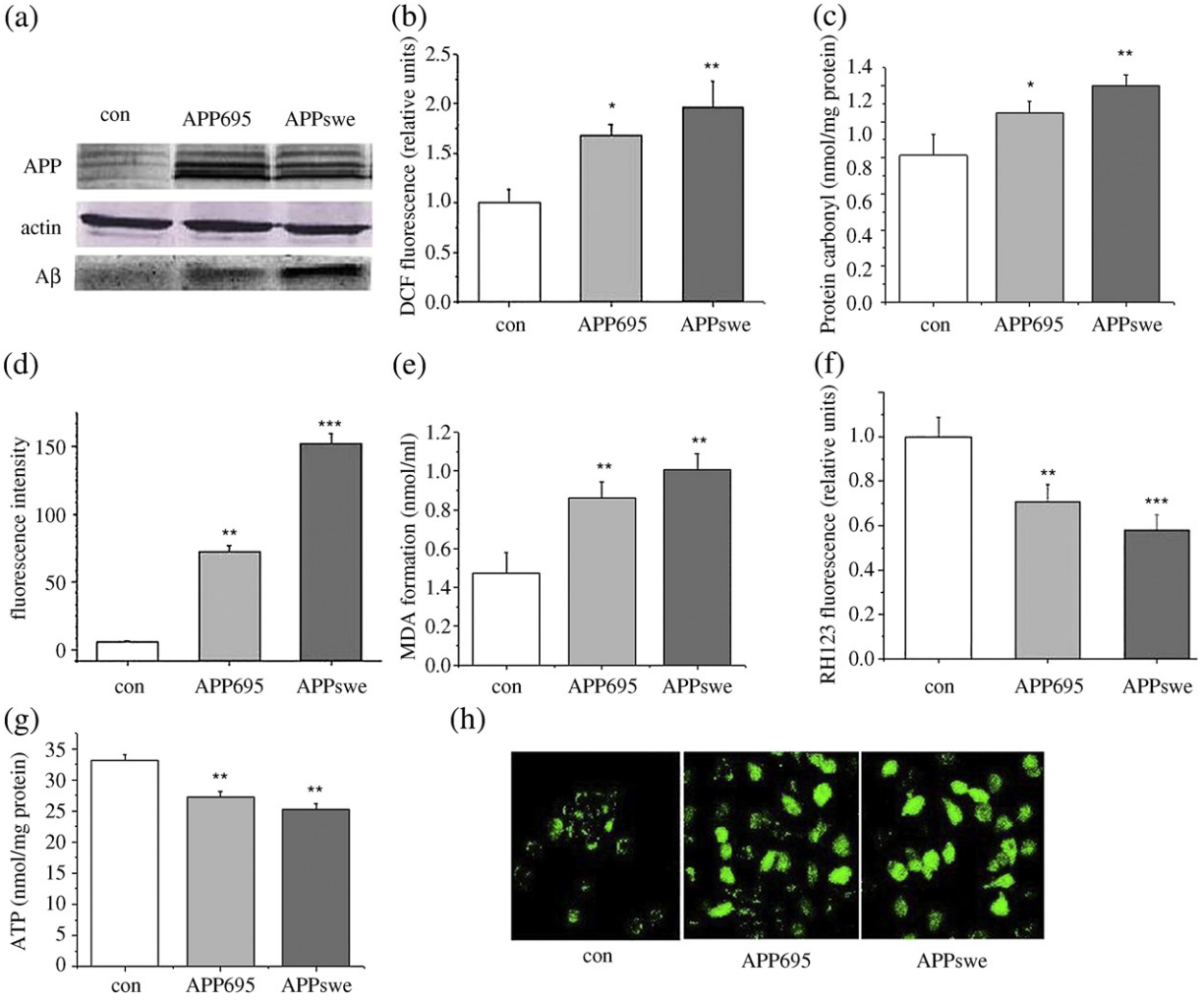

Fig. 1. Overexpression of wild type and Swedish mutant APP-induced oxidative stress, mitochondrial damage and calcium dysfunction. (a) The expression profile of APP was measured by Western blot analysis, and extracellular Aβ was measured by TCA precipitation in N2a/wt (con), N2a/APP695 and N2a/APPswe cells, respectively; (b) N2a/APP695 and N2a/APPswe cells showed increased intracellular ROS accumulation (ANOVA: **, $p<0.005$; *$p<0.05$ versus control cells); (c) Increase in protein carbonyls in N2a/APPwt and N2a/APPswe cells compared with control (con) cells (ANOVA: **, $p<0.005$; *$p<0.05$ versus control cells); (d) N2a/APP695 and N2a/APPswe cells exhibited a significant increase of basal NO levels compared to control cells (ANOVA: **, $p<0.005$; ***, $p<0.001$ versus control cells; (e) Level of malondialdehyde (MDA) was assayed according to the thiobarbituric acid method. Increase of MDA in N2a/APPwt and N2a/APPswe cells compared with control (con) cells (ANOVA: **, $p<0.005$ versus control N2a cells); (f) The mitochondrial membrane potential (Ψ_m) was significantly decreased in N2a/APP695 and N2a/APPswe cells compared with control cells (ANOVA: **, $p<0.005$, ***, $p<0.001$ versus control N2a cells); (g) ATP levels in N2a/APP695 and N2a/APPswe cells were significantly decreased compared to those in control cells (ANOVA: **, $p<0.005$ versus control N2a cells; (h) Increased intracellular calcium concentration in N2a/APP695 and N2a/APPswe cells compared with control cells was observed by confocal microscopy.

decrease in Ψ_m [26]. Indeed, there is evidence that over-expression of APP and its Swedish mutation result in impaired Ψ_m in HCN-1A neuronal cells [28] and PC12 cells [26].

To investigate whether endogenous Aβ was deleterious to the function of mitochondria in our model cells, we compared the Aβ model cells with wild type ones. As expected, N2a/APP695 and N2a/APPswe cells showed an obvious reduction in Ψ_m (Fig. 1f). Mitochondria are the major source of ATP. The level of ATP was determined in N2a/wt, N2a/APP695, and N2a/APPswe cells. The results indicated that the level of ATP in N2a/APP695 and N2a/APPswe cells was significantly decreased compared with those in N2a/wt cells ($P<0.005$ vs. control) (Fig. 1g). Excessive elevation of $[Ca^{2+}]_i$ is a major factor leading to apoptosis in many cell types. Degenerating neurons in the brains of AD patients showed increased levels of calcium [45,46]. Calcium dysregulation in AD also affects APP processing, endoplasmic reticulum (ER) dysfunction, and mitochondrial changes [47]. Here, N2a/wt, N2a/APP695, and N2a/APPswe cells were used to study the calcium dysregulation by measuring the level of $[Ca^{2+}]_i$. The results indicated that N2a/APP695, especially N2a/APPswe cells, showed higher intracellular fluorescence intensity, which demonstrated that $[Ca^{2+}]_i$ was significantly higher than in control cells (Fig. 1h).

N2a/Swe.D385A cells showed decreased basal levels of ROS, protein carbonyls, $[NO]_i$, and MDA

Asp-385 is required for presenilin 1 and γ-secretase activity. The loss-of-function PS1 mutant (D385A) leads to a deficiency in γ-secretase activity, while the FAD PS1 mutant (ΔE9) increases the activity of γ-secretase. Compared to N2a/Swe.ΔE9 and N2a/Swe.wt cells, N2a/Swe.D385A cells reduced Aβ secretion, and also increased the amount of holo-APP and the production of CTFs (Fig. 2A). In order to further demonstrate that oxidative stress is due to the increased endogenous Aβ but not due to the overexpression of APP and PS1, we compared the basal levels of $[NO]_i$, ROS and protein carbonyls in N2a/Swe.ΔE9, N2a/Swe.wt and N2a/Swe.D385A cells. We found that

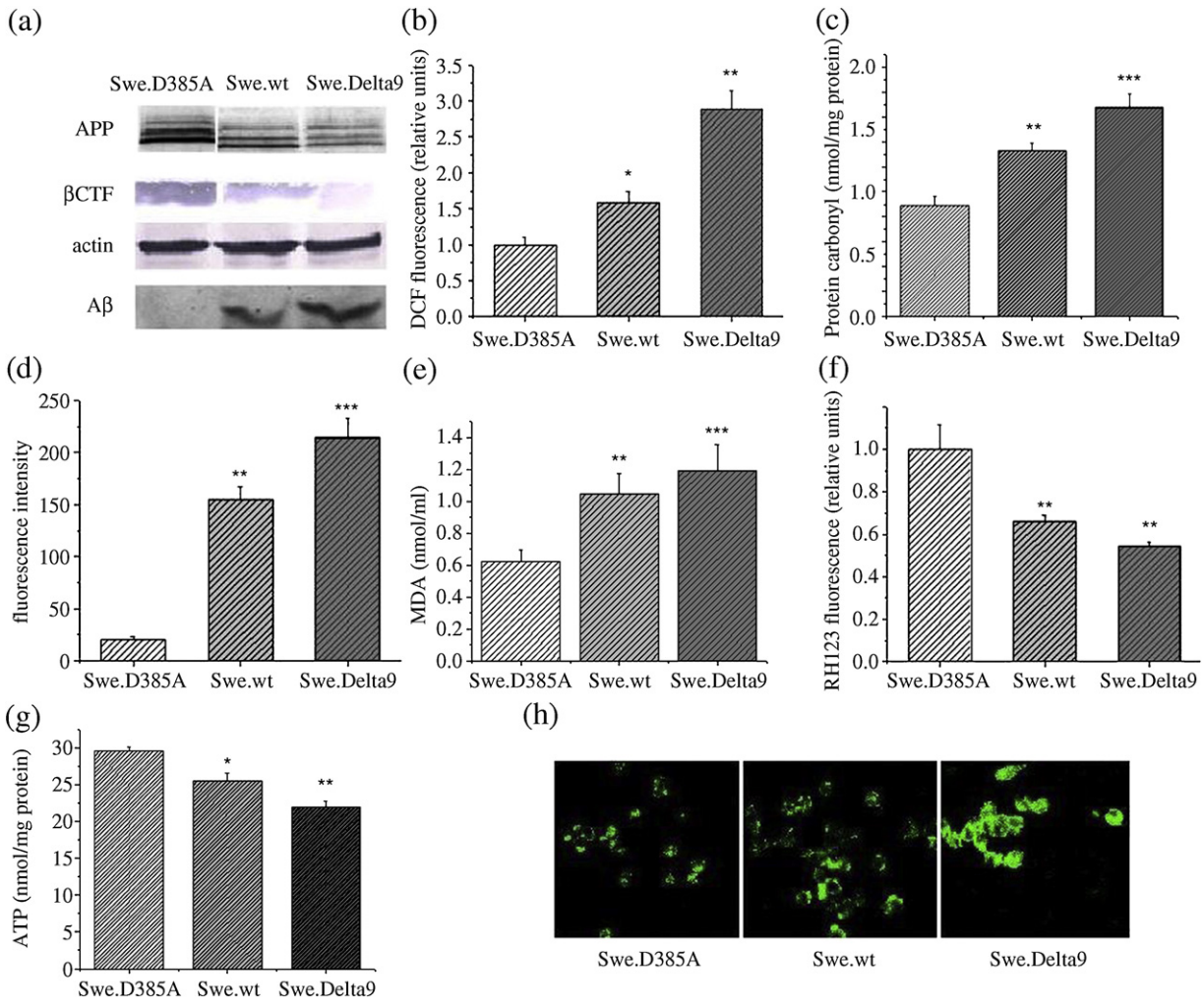

Fig. 2. Inhibition of γ-secretase by expressing PS1 D385A mutant protected cells from oxidative stress, mitochondrial damage and calcium dysfunction. (a) Expression profile of APP and APP C-terminal fragments were measured by Western blot analysis, and extracellular Aβ was measured by TCA precipitation in N2a/Swe.D385A, N2a/Swe.wt and N2a/Swe.ΔE9 cells. Compared to N2a/Swe.wt and N2a/Swe.ΔE9 cells, N2a/Swe.D385A cells showed higher levels of full length APP and C-terminal fragments, but the secreted Aβ was undetectable; (b) N2a/Swe.D385A cells showed reduced intracellular ROS accumulation compared to N2a/Swe.wt and N2a/Swe.ΔE9 cells (ANOVA: ** $p<0.005$ versus N2a/Swe.ΔE9; *$p<0.05$ versus N2a/Swe.wt cells; (c) Reduced protein carbonyls in N2a/Swe.D385A cells compared with those in N2a/Swe.wt and N2a/Swe.ΔE9 cells (ANOVA: ** $p<0.005$ versus N2a/Swe.ΔE9; *$p<0.05$ versus N2a/Swe.wt cells); (d) N2a/Swe.D385A cells exhibited significantly reduced basal NO levels compared to N2a/Swe.wt and N2a/Swe.ΔE9 cells (ANOVA: **, $p<0.005$ versus N2a/Swe.wt cells; ***, $p<0.001$ versus N2a/Swe.ΔE9); (e) N2a/Swe.D385A cells displayed decreased MDA level compared with N2a/Swe.wt and N2a/Swe.ΔE9 cells (**, $p<0.005$ versus N2a/Swe.wt cells; ***, $p<0.001$ versus N2a/Swe.ΔE9); (f) The mitochondrial membrane potential (Ψ_m) was significantly increased in N2a/Swe.D385A cells compared with N2a/Swe.wt and N2a/Swe.ΔE9 cells (ANOVA: **, $p<0.005$, versus N2a/Swe.wt and N2a/Swe.ΔE9 cells); (g) N2a/Swe.D385A cells displayed increased ATP level compared with N2a/Swe.wt and N2a/Swe.ΔE9 cells (ANOVA: ** $p<0.005$ versus N2a/Swe.ΔE9; *$p<0.05$ versus N2a/Swe.wt cells); (h) Reduced intracellular calcium concentration in N2a/Swe.D385A cells compared with that in N2a/Swe.wt and N2a/Swe.ΔE9 cells was observed by confocal microscopy.

in all cases, the levels of ROS (Fig. 2b), protein carbonyls (Fig. 2c) and $[NO]_i$ (Fig. 2d) were in the following order: N2a/Swe.D385A<N2a/Swe.wt<N2a/Swe.ΔE9. Besides, N2a/Swe.D385A cells showed obvious reduction of MDA level compared to N2a/Swe.wt, and N2a/Swe.ΔE9 cells (Fig. 2e). Together, these results suggested that the increased production of NO, ROS, protein carbonyls, and MDA in N2a/Swe.wt and N2a/Swe.ΔE9 cells were triggered by the production and accumulation of Aβ, and, impaired production of endogenous Aβ by the loss of PS1 function in the γ-cleavage of APP in N2a/Swe.D385A cells weakened the oxidative stress.

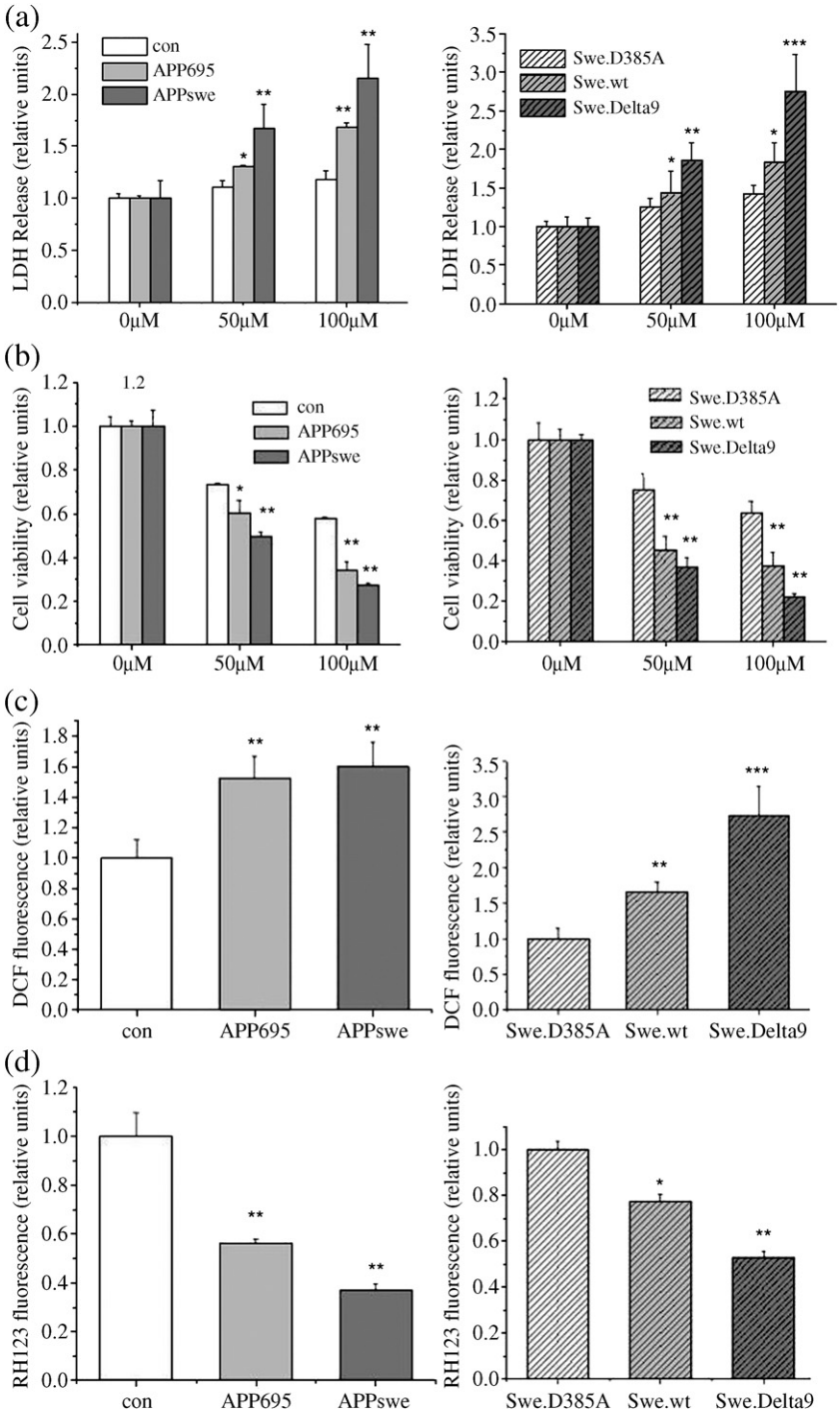

Fig. 3. LDH leakage, MTT reduction assay, ROS and mitochondrial membrane potential (Ψ_m) were used to evaluate the effect of secondary insult of oxidative stress on cells of different genotypes. (a) LDH release in N2a cells pretreated 24 h with H_2O_2 at concentrations of 50 μm and 100 μm. Results were shown as mean ± SEM obtained from five independent preparations (ANOVA: *, $p<0.05$ and **, $p<0.005$ versus N2a/wt cells, left panel; *, $p<0.05$, **, $p<0.005$**, and ***, $p<0.001$ versus N2a/Swe.D385A cells, right panel); (b) Cell viability was measured by MTT reduction assay after treatment with H_2O_2 for 24 h at concentrations of 50 μm and 100 μm. Results shown are mean ± SEM obtained from five independent preparations (ANOVA: *, $p<0.05$ and **, $p<0.005$ versus N2a/wt cells, left panel; **, $p<0.005$ versus N2a/Swe.D385A cells, right panel); (c) ROS was significantly increased in N2a/APP695 and N2a/APPswe (ANOVA: **, $p<0.005$ versus control cells, left panel) but significantly reduced in N2a/Swe.D385A compared to N2a/Swe.wt and N2a/Swe.ΔE9 cells (ANOVA: **, $p<0.005$ versus N2a/Swe.wt cells; ***, $p<0.001$ versus N2a/Swe.ΔE9, right panel); (d) Ψ_m was significantly increased in N2a/APP695 and N2a/APPswe (ANOVA: **, $p<0.005$ versus control cells, left panel) but significantly reduced in N2a/Swe.D385A compared to N2a/Swe.wt and N2a/Swe.ΔE9 cells (ANOVA: *, $p<0.05$ versus N2a/Swe.wt cells; ***, $p<0.005$ versus N2a/Swe.ΔE9 cells, right panel).

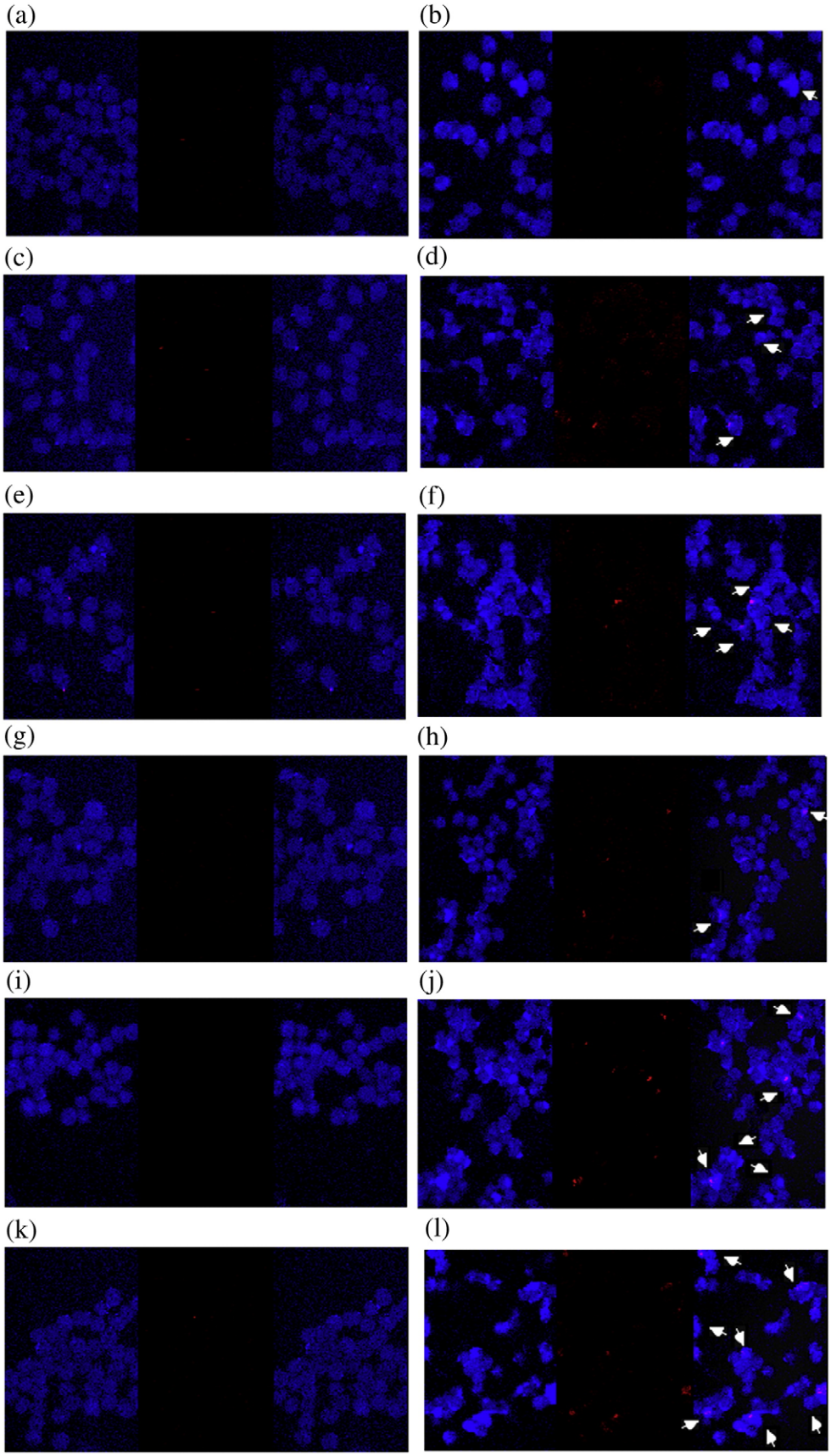

Fig. 4. H_2O_2-induced DNA fragmentation as determined by Hoechst PI staining. The arrowheads indicate the apoptotic bodies. Model cells were as follows: (a) N2a/wt; (b) N2a/wt+H_2O_2; (c) N2a/APP695; (d) N2a/APP695 H_2O_2; (e) N2a/APPswe (f) N2a/APPswe H_2O_2; (g) N2a/Swe.D385A; (h) N2a/Swe.D385A +H_2O_2; (i) N2a/Swe.wt; (j) N2a/Swe.wt+H_2O_2; (k) N2a/Swe.ΔE9; (l) N2a/Swe.ΔE9+H_2O_2.

N2a/Swe.D385A cells showed reversed mitochondrial damage and calcium dysfunction

A number of recent studies have indicated that mitochondria might be an important target of Aβ. Based on the observation above of oxidative stress, we supposed that when the production of Aβ was reduced in N2a/Swe.D385A cells, mitochondrial damage and calcium dysfunction would be lessened. To validate our hypothesis, we detected Ψ_m using fluorescence dye rhodamine123, ATP using bioluminescence assay, and $[Ca^{2+}]_i$ using fluo3/AM. As shown in Fig. 2f, N2a/Swe.D385A cells showed significantly higher Ψ_m than N2a/Swe.wt and N2a/Swe.ΔE9 cells. The mitochondrial function was resumed in N2a/Swe.D385A cells shown by increased level of ATP. The results indicated that the levels of ATP in N2a/Swe.wt, and, especially in N2a/Swe.ΔE9 cells, were significantly decreased compared with those in N2a/Swe.D385A cells (Fig. 2g). At the same time, it was shown that N2a/Swe.D385A cells displayed significantly lower $[Ca^{2+}]_i$ than N2a/Swe.wt and N2a/Swe.ΔE9 cells.

N2a/Swe.D385A cells showed reduced sensitivity to oxidative stress

Oxidative stress was observed in the AD brain. Oxidative stress occurs due to an imbalance in the prooxidant and antioxidant levels [48]. Increased production of ROS and free radicals might be involved in the pathology of AD. Thus, we investigated the effect of a secondary insult in the presence of an oxidative damage agent, hydrogen peroxide. Firstly, the integrity of cell membrane was determined by the release of LDH after 24 h exposure to 50 μM or 100 μM H_2O_2. As shown in Fig. 3a, after 24 h exposure to 50 μM or 100 μM H_2O_2, the N2a/APP695 and N2a/APPswe cells displayed markedly increased LDH leakage into the medium compared to control ones, while N2a/Swe.D385A cells showed reduced LDH efflux compared to N2a/Swe.wt and N2a/Swe.ΔE9 ones. Secondly, cell viability was evaluated by MTT after 24 h exposure to 50 μM or 100 μM H_2O_2. The N2a/APP695 and N2a/APPswe cells showed increased vulnerability compared to the control ones, while N2a/Swe.D385A cells showed reduced vulnerability compared to N2a/Swe.wt and N2a/Swe.ΔE9 ones (Fig. 3b). Then, after exposure to hydrogen peroxide, the ROS elevation was more pronounced in N2a/APP695 and N2a/APPswe cells compared to control ones, while N2a/Swe.D385A cells showed greater endurance to ROS elevation induced by hydrogen peroxide compared with N2a/Swe.wt and N2a/Swe.ΔE9 cells (Fig. 3c). Moreover, N2a/APP695 and N2a/APPswe cells showed a significantly decreased Ψ_m after exposure to hydrogen peroxide in comparison with control N2a cells. And N2a/Swe.D385A cells showed less reduction of Ψ_m than did the N2a/Swe.wt and N2a/Swe.ΔE9 cells (Fig. 3d).

Reduced vulnerability of N2a/Swe.D385A cells to H_2O_2 induced apoptosis

Using equal concentrations of H_2O_2, we investigated the apoptosis of different cell lines in response to oxidative stress. We examined apoptotic bodies by Hochest33258 and PI staining. After 24 h incubation with 50 μM H_2O_2, a significant proportion of the N2a/APP695 and N2a/APPswe cells had condensed and their nuclei had fragmented; these cells were stained more brightly than the control ones. For doubly transfected cells, N2a/Swe.ΔE9 cells showed the highest apoptotic and necrotic portion, and N2a/Swe.D385A cells displayed the lowest apoptotic and necrotic portion (Fig. 4).

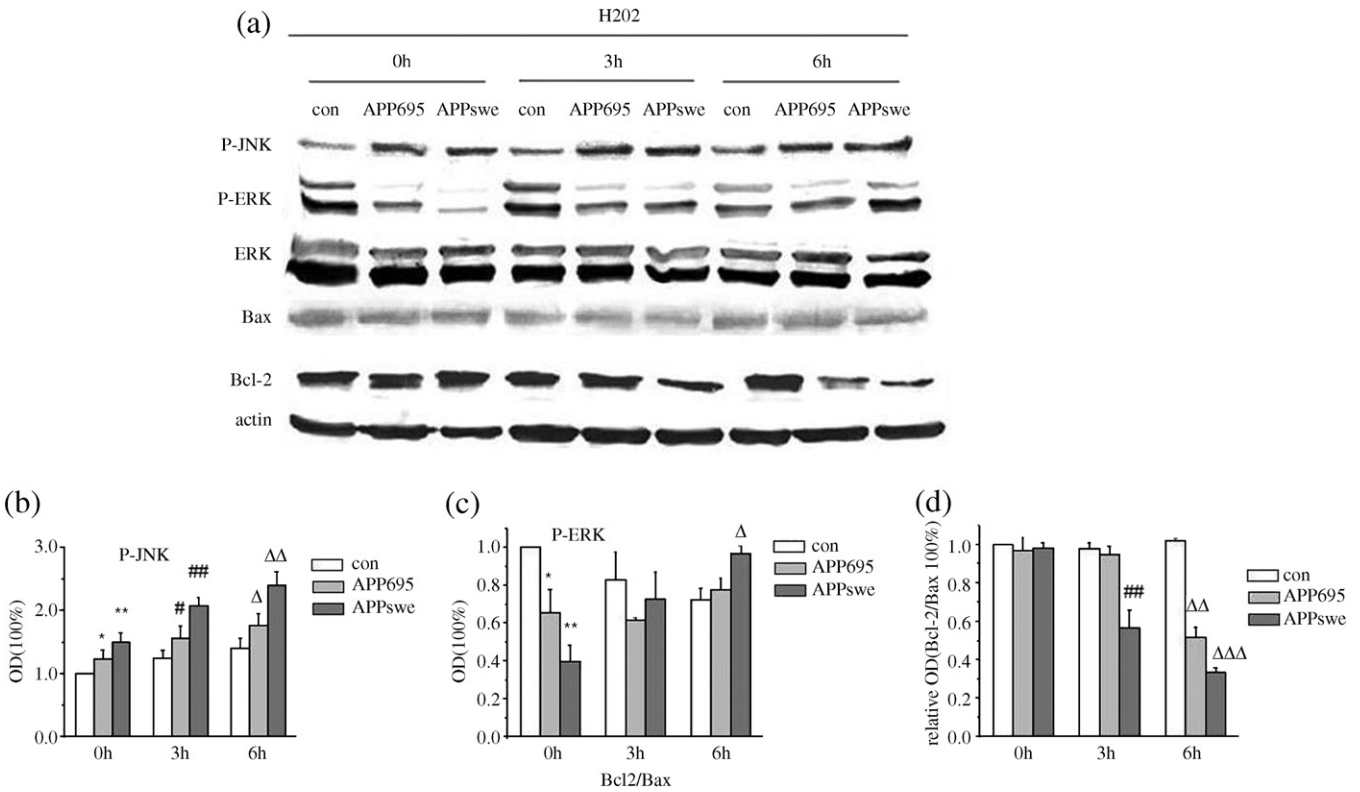

Fig. 5. (a) Changes in levels of P-JNK, P-ERK1/2, Bax and Bcl-2 after secondary insult of oxidative stress in N2a/wt, N2a/APP695 and N2a/APPswe cells; (b) N2a/APP695 and N2a/APPswe cells exhibited significantly enhanced protein expression levels of JNK activation compared with control cells with or without H_2O_2 treatment (ANOVA: **, $p<0.005$; *$p<0.05$ versus control cells); (c) The phosphorylation of ERK1/2 was reduced in N2a/APP695 and N2a/APPswe cells (**, $p<0.005$; *$p<0.05$ versus control cells), but there was a significant change in phosphorylation of ERK1/2 in N2a/APP695, especially in N2a/APPswe cells compared to wild type cells after H_2O_2 treatment; (d) We observed a significantly reduced shift in the Bcl-2 /Bax ratio in N2a/APP695 and N2a/APPswe cells after exposure to hydrogen peroxide (ANOVA: ##, $p<0.005$ versus control cells in 3 h; ΔΔ, $p<0.005$; ΔΔΔ, $p< 0.001$ versus control cells in 6 h).

Reduced activation of JNK and ERK pathways in N2a/Swe.D385A cells

Reactive oxygen species have been indicated to induce the activation of mitogen-activated protein kinases, including JNK, P38 and ERK. The JNK and P38 activation was observed to localize to amyloid deposits in AD model mice [49]. ERK activation was reported in hippocampal slices after treatment with soluble Aβ1-42 [50], though it was not found in AD model mice. Hence, we addressed the question of whether inhibiting abnormal γ-cleavage of APP could modulate MAPK family-involved apoptotic cell death in N2a cells. Interestingly, the endogenous JNK activity both at the basal state and in the H_2O_2-stimulated state was higher in N2a/APP695 and N2a/APPswe cells than that in control ones (Fig. 5a), while N2a/Swe.D385A cells reversed this elevation of JNK activity compared to N2a/Swe.wt and N2a/Swe.ΔE9 cells (Fig. 6a). Then we examined the activity of ERK. Surprisingly, we found the basal activity of ERK was significantly decreased in N2a/APP695 and N2a/APPswe cells compared to N2a/wt ones (Fig. 5a), and in N2a/Swe.D385A cells compared to N2a/Swe.wt and N2a/Swe.ΔE9 cells (Fig. 6a). After 3 h and 6 h treatment with 50 μM H_2O_2, a pathologic model of N2a cells showed an obviously increased phosphorylated level of ERK (Fig. 5a) (Fig. 6a), while the control (Fig. 5a) and N2a/Swe.D385A cells were only slightly influenced (Fig. 6a).

The impact of inhibiting γ-secretase abnormal cleavage of APP on Bcl-2 and Bax

Having established the mitochondrial damage during the process of H_2O_2-induced apoptosis, we set out to find whether there was any distinction between the effect of hydrogen peroxide on the pro-apoptotic and anti-apoptotic pathway. By western blot analysis, we monitored the protein expression of Bax (a pro-apoptotic member) and Bcl-2 (an anti-apoptotic member) following treatment of N2a cells by hydrogen peroxide. After 6 h of treatment with hydrogen peroxide, we found a reduced amount of the cytosolic anti-apoptotic protein Bcl-2 in N2a/APP695 cells and especially in N2a/APPswe cells (Fig. 5a). As far as doubly transfected cells were concerned, N2a/Swe.wt cells, and especially N2a/Swe.ΔE9 cells, showed significantly reduced levels of Bcl-2, whereas N2a/Swe.D385A cells showed only a minor change (Fig. 6a). Negligible changes in Bax protein content were observed in all of the cell lines (Figs. 5a and 6a). Thus, the Bcl-2/Bax ratio was obviously decreased in pathological cell models (Figs. 5d and 6d), but not in N2a/wt and N2a/Swe.D385A cells (Fig. 6d). All the above apoptosis studies suggest that, in the presence of an oxidative damage-inducing agent, inhibition of abnormal cleavage of APP by γ-secretase helped to resist apoptosis.

Aβ level positively correlated with ROS levels and mitochondrial damage

Having demonstrated a significant increase in ROS and mitochondrial damage with endogenous Aβ, we postulated that the production of ROS and mitochondrial damage is positively correlated with the Aβ level. To test this idea, we treated N2a/APP695 and N2a/APPswe cells for 24 h with a low concentration of butyric acid [51] to induce overexpression of the transfected genes. As shown in Fig. 7b, the ROS level increased after the treatment, concomitantly with increased APP and Aβ levels (Fig.7a). At the same time, the levels of Ψ_m and ATP were detected. After treatment with butyric acid, both N2a/APP695 and N2a/APPswe cells showed a significant reduction of Ψ_m (fig.7c) and ATP (fig.7d) which showed the dose-dependent effects of Aβ on cellular damage. To further demonstrate the deleterious effect of endogenous Aβ, N2a/APP695 and N2a/APPswe cells were treated with DAPT, a functional γ-secretase inhibitor that reduces

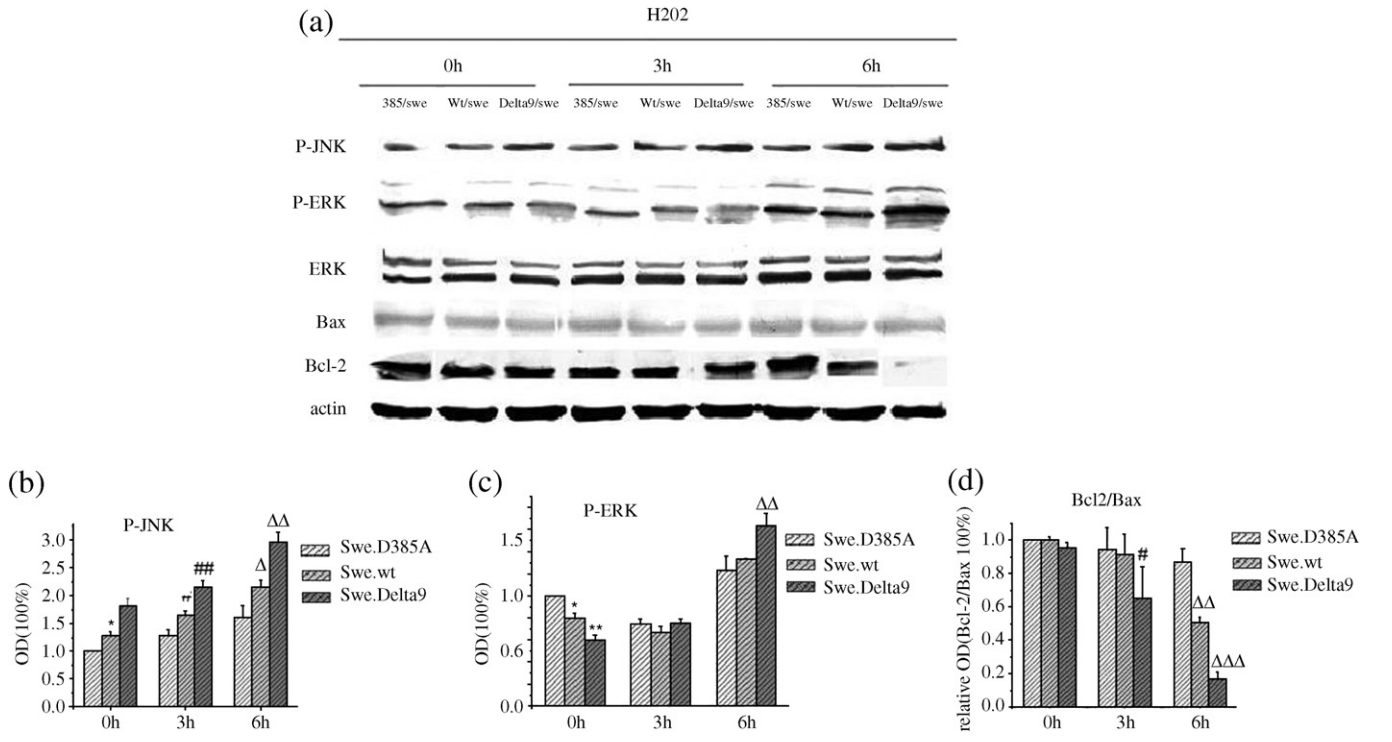

Fig. 6. (a) Changes in levels of P-JNK, P-ERK1/2, Bax and Bcl-2 after secondary insult of oxidative stress in N2a/Swe.D385A, N2a/Swe.wt and N2a/Swe.ΔE9 cells; (b) N2a/Swe.wt and N2a/Swe.ΔE9 cells exhibited significantly enhanced protein expression levels of JNK activation compared with N2a/Swe.D385A cells with or without H_2O_2 treatment (ANOVA: **, $p<0.005$; *$p<0.05$ versus control cells); (c) The phosphorylation of ERK1/2 was reduced in N2a/Swe.wt and N2a/Swe.ΔE9 cells (**, $p<0.005$; *$p<0.05$ versus N2a/Swe.D385A cells), but there was a significant change in phosphorylation of ERK1/2 in N2a/Swe.wt, especially in N2a/Swe.ΔE9 cells compared to N2a/Swe.D385A cells after H_2O_2 treatment; (d) We observed a significantly reduced shift in the Bcl-2 /Bax ratio in N2a/Swe.wt and N2a/Swe.ΔE9 cells after exposure to hydrogen peroxide (ANOVA: ##, $p<0.005$ versus N2a/Swe.D385A cells in 3 h; ΔΔ, $p<0.005$; ΔΔΔ, $p< 0.001$ versus N2a/Swe.D385A cells in 6 h).

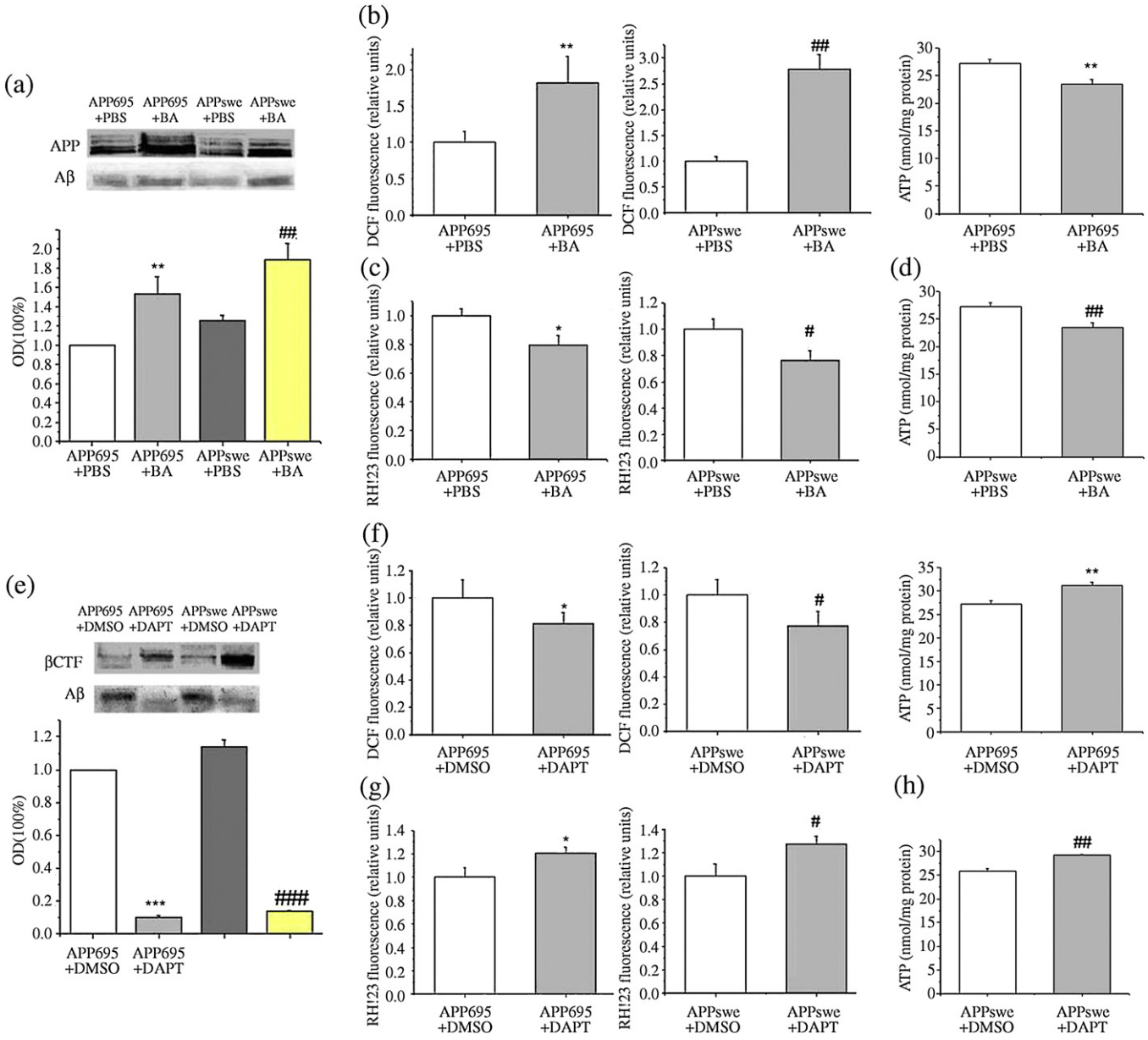

Fig. 7. Neurotoxicity was positively correlated with Aβ level, and the γ-secretase inhibitor DAPT reduced ROS levels and restored mitochondrial activity. (a) N2a/APP695 and N2a/APPswe cells were incubated in the presence or absence of 5 mM butyric acid (BA) for 24 h to induce APP expression and Aβ secretion. Levels of Aβ were quantified and normalized to those of N2a/APP 695 cells without BA treatment (AVOVA: ** $p<0.005$ versus untreated N2a/APP695 cells; ##, $p<0.005$ versus untreated N2a/APPswe cells); (b) The ROS level was significantly increased in both N2a/APP695 (AVOVA: ** $p<0.005$ versus untreated N2a/APP695 cells) and N2a/APPswe cells (AVOVA: ##, $p<0.005$ versus untreated N2a/APPswe cells) after treatment with BA; (c) Ψ_m was significantly reduced in both N2a/APP695 (AVOVA: *, $p<0.05$ versus untreated N2a/APP695 cells) and N2a/APPswe cells (AVOVA: #, $p<0.005$ versus untreated N2a/APPswe cells) after treatment with BA; (d) ATP level was significantly reduced in both N2a/APP695 (AVOVA: **, $p<0.005$ versus untreated N2a/APP695 cells) and N2a/APPswe cells (AVOVA: ##, $p<0.005$ versus untreated N2a/APPswe cells) after treatment with BA; (e) N2a/APP695 and N2a/APPswe cells were incubated in the presence of 250 nm DAPT. β-CTF and Aβ were detected. Aβ level was densitometrically analyzed (AVOVA: *** $p<0.001$ versus untreated N2a/APP695 cells; ###, $p<0.001$ versus untreated N2a/APPswe cells); (f) The ROS level was significantly reduced in both N2a/APP695 (AVOVA: * $p<0.05$ versus untreated N2a/APP695 cells) and N2a/APPswe cells (AVOVA: #, $p<0.05$ versus untreated N2a/APPswe cells) after treatment with DAPT; (g) Ψ_m was significantly increased in both N2a/APP695 (AVOVA: * $p<0.05$ versus untreated N2a/APP695 cells) and N2a/APPswe cells (AVOVA: #, $p<0.05$ versus untreated N2a/APPswe cells) after treatment with DAPT; (h) ATP level was significantly increased in both N2a/APP695 (AVOVA: **, $p<0.005$ versus untreated N2a/APP695 cells) and N2a/APPswe cells (AVOVA: ##, $p<0.005$ versus untreated N2a/APPswe cells) after treatment with DAPT.

intracellular Aβ. An obvious increase of βCTF and reduction of secreted Aβ was detected by TCA precipitation after 24 h treatment of DAPT (Fig. 7e). DAPT led to a significantly reduced ROS level (Fig. 7f) as well as a strongly increased Ψ_m in both N2a/APP695 and N2a/APPswe cells (Fig. 7 g). Moreover, N2a/APP695 and N2a/APPswe cells showed increased level of ATP after treatment with DAPT (Fig. 7h). Thus, we proved that inhibition of Aβ by exogenous γ-secretase inhibitor led to a decrease in ROS level and a stabilization of mitochondrial function, which coincided with the endogenous gene mutant results.

Effects of anti Aβ antibodies on ROS and Ψ_m in N2a/Swe.ΔE9 cells

N2a/Swe.D385A cells secreted little Aβ, while N2a/Swe.ΔE9 cells secreted abundant Aβ. To verify if Aβ was the cause of cell damage in N2a pathologically model cells, 0.05% Aβ monoclonal antibody 4G8 and anti Aβ serum were added into the culture medium of N2a/Swe.D385A cells and N2a/Swe.ΔE9 cells independently. 24 hours after the treatment, the levels of ROS and Ψ_m were determined. The results showed that both Aβ antibody 4G8 and anti Aβ serum decreased the level of ROS in N2a/Swe.ΔE9 cells (Fig. 8a), while not in N2a/Swe.

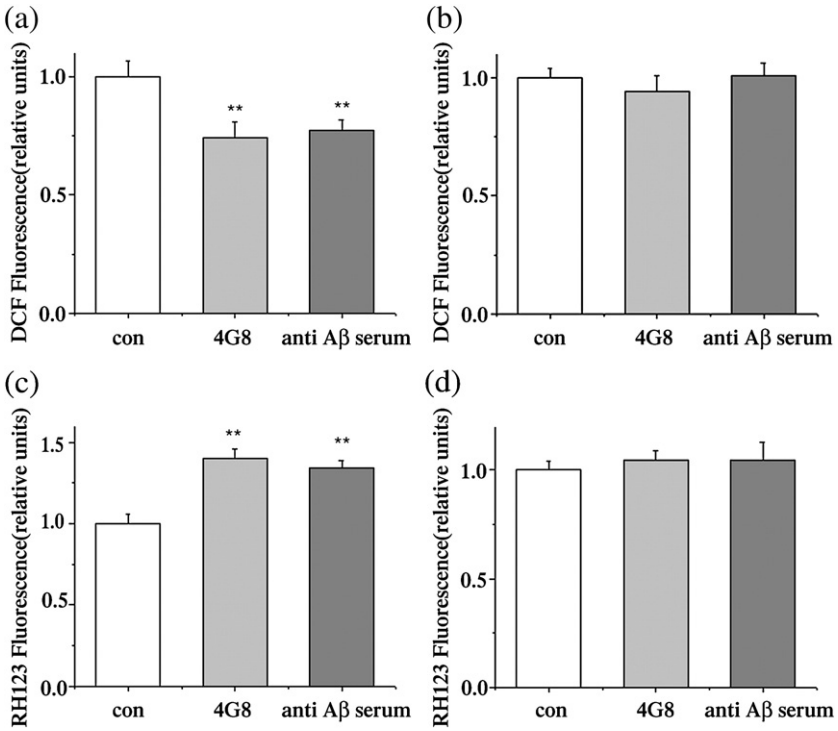

Fig. 8. Aβ antibody and antiserum prevented increase of ROS and reduction of mitochondrial membrane potential in N2a/Swe. ΔE9 cells but not in N2a/Swe.D385A cells. (a) ROS was significantly reduced in N2a/Swe.ΔE9 cells after treatment with Aβ monoclonal antibody 4G8 and Aβ antiserum (ANOVA: **, $p<0.005$); (b) ROS nearly kept constant in N2a/Swe. D385A after treatment with Aβ antibody 4G8 and Aβ antiserum; (c) Ψ_m was significantly increased in N2a/Swe.ΔE9 cells after treatment with Aβ monoclonal antibody 4G8 and Aβ antiserum (ANOVA: **, $p<0.005$); (d) Ψ_m was nearly kept constant in N2a/Swe.D385A after treatment with Aβ antibody 4G8 and Aβ antiserum.

D385A cells (Fig. 8b). Correspondingly, N2a/Swe.ΔE9 cells showed a markedly increased Ψ_m after treatment with the Aβ antibody 4G8 and anti Aβ serum (Fig. 8c), while the level of Ψ_m kept almost constant after 4G8 and anti Aβ serum treatment in N2a/Swe.D385A cells (Fig. 8d). It demonstrated that cell damage in N2a/Swe.ΔE9 was mainly caused by Aβ overproduction. And reduced production of Aβ was the reason for the reduction of ROS formation and increase of Ψ_m in N2a/Swe. D385A cells.

Discussion

The overproduction and accumulation of Aβ-peptide in the brain has been considered as the central pathological event in AD. Genetic mutations in genes for APP, presenilin-1 or presenilin-2 have been reported to increase the production of Aβ42 and lead to early onset of AD [52]. Many therapeutic strategies have been proposed based on Aβ biology [53]. Several studies showed that β- and γ-secretase is a promising pharmacological target as a means to interfere with the production of Aβ. Many γ-secretase inhibitors have been tested in laboratories or clinical experiments [54,55]. However, strong inhibition of γ-secretase leads to severe adverse effects, as it interferes with signaling by notch proteins and other cell surface receptors [56]. Thus, it has been debated whether using γ-secretase inhibitor to treat AD is secure enough. A recent study concluded that a γ-secretase reduction of 30% was sufficient to attenuate Aβ deposition with little or no adverse side effects, suggesting the existence of an optimal window of therapeutic γ-secretase inhibition [34]. It was reported that expression of PS1 harboring alanine substitutions of highly conserved aspartate residue at position 385 in Chinese hamster ovary cells [57] or N2a cells [36] led to reduced Aβ secretion and accumulation of APP CTFs. Intrigued with this observation, our research objective was to explore the feasibility of γ-secretase inhibition. In this report, we offered several important insights into the changes induced by the PS1 D385A variant on oxidative stress, mitochondrial damage and apoptosis.

Oxidative stress and mitochondrial damage are known to occur in the AD brain. Our data showed that N2a/APP695 and N2a/APPswe cells exhibited increased basal levels of NO, ROS, protein carbonyls and MDA, which play important roles in Aβ-induced neurotoxicity and cell death. Previous study showed that increased oxidative damage was an early event in AD, and increases in Aβ deposition were associated with decreased oxidative damage. They suggested that AD was associated with compensatory changes that reduced damage from reactive oxygen [58]. This result didn't deny the positive correlation between Aβ production and oxidative stress. It is widely believed that soluble Aβ oligomers (Aβ-derived diffusible ligands, ADDLs) are more toxic than insoluble Aβ polymers [59]. Aβ deposition transforms soluble Aβ oligomers into insoluble precipitate of Aβ polymers. Therefore, Aβ deposition could be a compensatory response to toxic effects, including oxidative stress, induced by overproduced soluble Aβ oligomers. Increased oxidative stress was consistent with the observation that the sensitivities to oxidative stress induced by H_2O_2 in N2a/APP695, especially in N2a/APPswe cells, were significantly promoted compared with control cells. Oxidative stress also plays a key role in the Aβ-mediated neurotoxicity. It was reported that H_2O_2 participated in mediating Aβ toxicity [60] and Aβ could directly produce H_2O_2 through metal ion reduction [61]. These results enhanced our understanding of Aβ central pathology. We also investigated the effects on oxidative stress and mitochondrial damage of reduced production of Aβ by inhibiting γ-secretase. When cells were co-transfected with Swedish mutant APP and PS1 dominant negative mutant (PS1D385A), no secreted Aβ was detected by TCA precipitation. Compared to N2a/Swe.wt and N2a/Swe.ΔE9 cells, N2a/Swe.D385A cells showed reduced neurotoxicity, including levels of NO, ROS, protein carbonyls and mitochondrial dysfunction. Moreover, when treated with a secondary insult (H_2O_2), N2a/Swe.D385A cells displayed stronger resistance and could better maintain cellular function. The results of this study supported the hypothesis that there was a reduced basal neurotoxicity and sensibility to oxidative stress

when PS1 activity was inhibited. Oxidative stress and Aβ production are positively correlated to each other. There is evidence suggesting that Aβ induces oxidative stress both in vivo and in vitro [62,63], and oxidative stress promotes the production of Aβ [64]. A recent study [65] showed that oxidative stress induced by H_2O_2 and HNE treatments activated a positive feedback between the γ- and β-secretase cleavages of the β-amyloid precursor protein, which led to an increase in Aβ40 and Aβ42 production as well as Aβ42/40 ratios. This kind of feedback required the activation of the JNK/c-jun pathway. Combined with our results, it seemed that when the γ-secretase activity was inhibited in N2a/Swe.D385A cells, the positive feedback could not be observed. Moreover, the effects on cellular ROS, Ψ_m and ATP of DAPT were a supplementary result.

Apoptosis is attributed to neurodegenerative diseases and neurological disorders, such as AD and Parkinson's disease. Increased levels of ROS and mitochondrial dysfunction are involved in Aβ-induced apoptosis [66]. Studies have established that Aβ peptide induces apoptosis in mouse neuronal cultures [67]. Familial AD (FAD) mutations in presenilins render neurons vulnerable to apoptosis induced by Aβ [68]. Consistent with previous studies, we found that N2a/APP695 and N2a/APPswe cells, which have high Aβ levels, showed significantly increased proportions of apoptotic cells after treatment with 50 μM H_2O_2. As the MAPK pathway has been found to play a role in AD pathology [25,69], we found that after treatment with H_2O_2 for 3 h and 6 h, N2a/APP695 and N2a/APPswe cells exhibited significantly enhanced protein expression levels of ERK and JNK activation compared to control cells. This result suggested that the endogenous Aβ might promote the activation of JNK and ERK induced by oxidative stress. Furthermore, this effect is Aβ dose-dependent. Given the important relationship between Aβ and apoptosis, we investigated the influence on apoptosis when the activity of γ-secretase was inhibited by transfection with PS1 dominant negative mutant. Interestingly, we observed that N2a/Swe.D385A cells, which secreted little Aβ, displayed significantly reduced proportions of apoptotic cells after treatment with 50 μM H_2O_2 compared to N2a/Swe.wt and N2a/Swe.ΔE9 cells. At the same time, we found that expression of the D385A PS1variant retarded activation of the JNK and ERK1/2 pathways. Both ERK1/2 and JNK pathways are generally activated in susceptible neuronal populations in individuals with AD. And there is evidence suggesting that the activation of ERK and JNK can independently serve to initiate, but both are necessary to propagate disease pathogenesis [70]. They called this “two hits hypothesis” [71]. And they indicated that only with “two hits” could the disease process be started.” Combined with our results, we speculated that oxidative stress, as an early event in AD, played an important role in activating ERK1/2 and JNK pathways. It was shown that when γ-secretase activity was inhibited in N2a/Swe.D385A cells, the “two hits” was delayed.

Though the expression of Bax stayed consistent, a shift in the Bcl-2/Bax ratio toward Bax might be involved in the different sensitivity of the three cell lines after secondary stress insult. We speculate that both reduced Aβ production and depressed oxidative stress lead to reduced vulnerability to apoptotic cell death.

External applied Aβ monoclonal antibody could bind the extracellular Aβ. The level of ROS could be decreased and Ψ_m could be increased in the presence of Aβ antibody in N2a/Swe.ΔE9 cells while not in N2a/Swe.D385A cells, which demonstrated that the extracellularly secreted Aβ played an important role in cell damages mentioned above. A recent study showed that extracellular fluorescent Aβ could be taken up by human SH-SY5Y neuroblastoma cells and later partly localized to mitochondria [72]. Besides, Saavedra and colleagues [73] have proved that Aβ42 is internalized by primary neurons in the absence of ApoE. These results implied that secreted Aβ could be reinternalized into cells and came in contact with mitochondria. Combined with our data, we speculated that Aβ, including the intracellular and the reinternalized extracellular, led to intracellular toxicity, including oxidative stress, mitochondrial dysfunction, and apoptosis. In accordance with our results, primary neuronal cultures from knock-in mice expressing mutant human PS-1 and APP neurons exhibited increased vulnerability to oxidative stress, mitochondrial dysfunction and apoptosis in the presence of Aβ42 compared with the wild-type neurons [16]. SH-SY5Y cells pretreated with Aβ antibody significantly prevented the cell neurotoxicity induced by Aβ [74].

In summary, compared to AD pathological cell models, N2a/Swe.D385A cells showed reduced oxidative stress, increased mitochondrial activity and decreased vulnerability to apoptosis. Thus, our data support the view that γ-secretase is a therapeutic target for treatment of AD. Optimum γ-secretase inhibitors, especially APP-specific γ-secretase inhibitors, are a good choice. However, additional work is required to understand the long-term effect associated with γ-secretase inhibitors.

Acknowledgments

We are grateful to Dr. H.X. Xu from the Burnham Institute for providing the N2a cell lines and antibodies. This work was supported by grants from the Tsinghua-Yue-Yuen Medical Sciences Fund (No. 20240000514), the National Natural Science Foundation of China (No. 30872898) and the "86.3" program of China (No. 2007AA02Z402 and 2008AA022403).

References

[1] Goedert, M.; Spillantini, M. G. A Century of Alzheimer's Disease. *Science* **314:** 777–781; 2006.
[2] Kidd, M. Paired helical filaments in electron microscopy of Alzheimer's disease. *Nature* **197:**192–193; 1963.
[3] Terry, R. D.; Gonatas, N. K.; Weiss, M. Ultrastructural Studies in Alzheimer's Presenile Dementia. *Am J Pathol.* **44:**269–297; 1964.
[4] Roher, A.; Wolfe, D.; Palutke, M.; KuKuruga, D. Purification, ultrastructure, and chemical analysis of Alzheimer's disease amyloid plaque core protein. *Proc Natl Acad Sci USA.* **83:**2662–2666; 1986.
[5] LaFerla, F. M.; Oddo, S. Alzheimer's disease: Aβ, tau and synaptic dysfunction. *Trends Mol Med.* **11:**170–176; 2005.
[6] Sherrington, R.; Rogaev, E. I.; Liang, Y.; Rogaeva, E. A.; Levesque, G.; Ikeda, M.; Chi, H.; Lin, C.; Li, G.; Holman, K. Cloning of a gene bearing missense mutations in early-onset familial Alzheimer's disease. *Nature* **375:**754–760; 1995.
[7] Hardy, J. A.; Higgins, G. A. Alzheimer's disease: the amyloid cascade hypothesis. *Science* **256:**184–185; 1992.
[8] Mattson, M. P. Pathways towards and away from Alzheimer's disease. *Nature* **430:** 631–639; 2004.
[9] Lee, H. G.; Casadesus, G.; Zhu, X.; Takeda, A.; Perry, G.; Smith, M. A. Challenging the amyloid cascade hypothesis: senile plaques and amyloid-β as protective adaptations to Alzheimer disease. *Ann. N.Y. Acad. Sci.* **1019:**1–4; 2004.
[10] Hirai, K.; Aliev, G.; Nunomura, A.; Fujioka, H.; Russell, R. L.; Atwood, C. S.; Johnson, A. B.; Kress, Y.; Vinters, H.; Tabaton, M.; Shimohama, S.; Cash, A. D.; Siedlak, S. L.; Harris, P. L.; Jones, P. K.; Petersen, R. B.; Perry, G.; Smith, M. A. Mitochondrial abnormalities in Alzheimer's disease. *J. Neurosci.* **21:**3017–3023; 2001.
[11] Butterfield, D. A.; Drake, J.; Pocernich, C.; Castegna, A. Evidence of oxidative damage in Alzheimer's disease brain: central role for amyloid β-peptide. *Trends Mol. Med.* **7:**548–554; 2001.
[12] Smith, M. A.; Harris, P. L.; Sayre, L. M.; Perry, G. Iron accumulation in Alzheimer's disease is a source of redox-generated free radicals. *Proc. Natl Acad. Sci. U. S. A.* **94:** 9866–9868; 1997.
[13] Castegna, A.; Aksenov, M.; Aksenova, M.; Thongboonkerd, V.; Klein, J. B.; Pierce, W. M.; Booze, R.; Markesbery, W. R.; Butterfield, D. A. Proteomic identification of oxidatively modified proteins in Alzheimer's disease brain. Part I. Creatine kinase BB, glutamine synthase, and ubiquitin carboxyterminal hydrolase L-1. *Free Radic. Biol. Med.* **33:**562–571; 2002.
[14] Castegna, A.; Thongboonkerd, V.; Klein, J. B.; Lynn, B.; Markesbery, W. R.; Butterfield, D. A. Proteomic identification of nitrated proteins in Alzheimer's disease brain. *J. Neurochem.* **85:**1394–1401; 2003.
[15] Castegna, A.; Thongboonkerd, V.; Klein, J.; Lynn, B. C.; Wang, Y. L.; Osaka, H.; Wada, K.; Butterfield, D. A. Proteomic analysis of brain proteins in the gracile axonal dystrophy (gad) mouse, a syndrome that emanates from dysfunctional ubiquitin carboxyl-terminal hydrolase L-1 reveals oxidation of key proteins. *J. Neurochem.* **88:**1540–1546; 2004.
[16] Mohmmad Abdul, H.; Sultana, R.; Keller, J. N.; St Clair, D. K.; Markesbery, W. R.; Butterfield, D. A. Mutations in amyloid precursor protein and presenilin-1 genes increase the basal oxidative stress in murine neuronal cells and lead to increased sensitivity to oxidative stress mediated by amyloid β-peptide (1-42), H2O2 and kainic acid: implications for Alzheimer's disease. *J. Neurochem.* **96:**1322–1335; 2006.

[17] Butterfield, D. A.; Reed, T.; Newman, S. F.; Sultana, R. Roles of amyloid β-peptide-associated oxidative stress and brain protein modifications in the pathogenesis of Alzheimer's disease and mild cognitive impairment. *Free Radic. Biol. Med.* **43:** 658–677; 2007.

[18] Casley, C. S.; Canevari, L.; Land, J. M.; Clark, J. B.; Sharpe, M. A. β-amyloid inhibits integrated mitochondrial respiration and key enzyme activities. *J. Neurochem.* **80:** 91–100; 2002.

[19] Sarti, P.; Arese, M.; Giuffrè, A. The molecular mechanisms by which nitric oxide controls mitochondrial complex IV. *Ital. J. Biochem. (Engl. Ed.)* **52:**37–42; 2003.

[20] Radi, R.; Cassina, A.; Hodara, R.; Quijano, C.; Castro, L. Peroxynitrite reactions and formation in mitochondria. *Free Radic. Biol. Med.* **33:**1451–1464; 2002.

[21] Keller, J. N.; Guo, Q.; Holtsberg, F. W.; Bruce-Keller, A. J.; Mattson, M. P. Increased sensitivity to mitochondrial toxin-induced apoptosis in neural cells expressing mutant presenilin-1 is linked to perturbed calcium homeostasis and enhanced oxy-radical production. *J. Neurosci.* **18:**4439–4450; 1998.

[22] Parola, M.; Robino, G.; Marra, F.; Pinzani, M.; Bellomo, G.; Leonarduzzi, G.; Chiarugi, P.; Camandola, S.; Poli, G.; Waeg, G.; Gentilini, P.; Dianzani, M. U. HNE interacts directly with JNK isoforms in human hepatic stellate cells. *J. Clin. Invest.* **102:**1942–1950; 1998.

[23] Soh, Y.; Jeong, K. S.; Lee, I. J.; Bae, M. A.; Kim, Y. C.; Song, B. J. Selective activation of the c-Jun N-terminal protein kinase pathway during 4-hydroxynonenal-induced apoptosis of PC12 cells. *Mol. Pharmacol.* **58:**535–541; 2000.

[24] Kurata, S. Selective activation of p38 MAPK cascade and mitotic arrest caused by low level oxidative stress. *J. Biol. Chem.* **275:**23413–23416; 2000.

[25] Marques, C. A.; Keil, U.; Bonert, A.; Steiner, B.; Haass, C.; Muller, W. E.; Eckert, A. Neurotoxic mechanisms caused by the Alzheimer's disease-linked Swedish amyloid precursor protein mutation: oxidative stress, caspases, and the JNK pathway. *J. Biol. Chem.* **278:**28294–28302; 2003.

[26] Keil, U.; Bonert, A.; Marques, C. A.; Scherping, I.; Weyermann, J.; Strosznajder, J. B.; Müller-Spahn, F.; Haass, C.; Czech, C.; Pradier, L.; Müller, W. E.; Eckert, A. Amyloid β-induced Changes in Nitric Oxide Production and Mitochondrial Activity Lead to Apoptosis. *J. Biol. Chem.* **279:**50310–50320; 2004.

[27] Tamagno, E.; Parola, M.; Guglielmotto, M.; Santoro, G.; Bardini, P.; Marra, L.; Tabaton, M.; Danni, O. Multiple signaling events in amyloid β-induced, oxidative stress-dependent neuronal apoptosis. *Free Radic. Biol. Med.* **35:**45–58; 2003.

[28] Anandatheerthavarada, H. K.; Biswas, G.; Robin, M. A.; Avadhani, N. G. Mitochondrial targeting and a novel transmembrane arrest of Alzheimer's amyloid precursor protein impairs mitochondrial function in neuronal cells. *J. Cell Biol.* **161:**41–54; 2003.

[29] Caspersen, C.; Wang, N.; Yao, J.; Sosunov, A.; Chen, X.; Lustbader, J. W.; Xu, H. W.; Stern, D.; McKhann, G.; Yan, S. D. Mitochondrial Aβ: a potential focal point for neuronal metabolic dysfunction in Alzheimer's disease. *FASEB J.* **19:**2040–2041; 2005.

[30] Manczak, M.; Anekonda, T. S.; Henson, E.; Park, B. S.; Quinn, J.; Reddy, P. H. Mitochondria are a direct site of Aβ accumulation in Alzheimer's disease neurons: implications for free radical generation and oxidative damage in disease progression. *Hum. Mol. Genet.* **15:**1437–1449; 2006.

[31] Takeda, K.; Araki, W.; Tabira, T. Enhanced generation of intracellular Aβ42 amyloid peptide by mutation of presenilins PS1 and PS2. *Eur. J. Neurosci.* **19:**258–364; 2006.

[32] Tienari, P. J.; Ida, N.; Ikonen, E.; Simons, M.; Weidemann, A.; Multhaup, G.; Masters, C. L.; Dotti, C. G.; Beyreuther, K. Intracellular and secreted Alzheimer's amyloid β species are generated by distinct mechanism in cultured hippocampal neurons. *Proc. Natl. Acad. Sci. U. S. A.* **94:**4125–4130; 1997.

[33] Bentahir, M.; Nyabi, O.; Verhamme, J.; Tolia, A.; Horré, K.; Wiltfang, J.; Esselmann, H.; De Strooper, B. Presenilin clinical mutations can affect gamma-secretase activity by different mechanisms. *J. Neurochem.* **96:**732–742; 2006.

[34] Li, T.; Wen, H.; Brayton, C.; Laird, F. M.; Ma, G.; Peng, S.; Placanica, L.; Wu, T. C.; Crain, B. J.; Price, D. L.; Eberhart, C. G.; Wong, P. C. Moderate reduction of γ-secretase attenuates amyloid burden and limits mechanism-based liabilities. *J. Neurosci.* **27:**10849–10859; 2007.

[35] Kim, S. H.; Leem, J. Y.; Lah, J. J.; Slunt, H. H.; Levey, A. I.; Thinakaran, G.; Sisodia, S. S. Multiple effects of aspartate mutant presenilin 1 on the processing and trafficking of amyloid precursor protein. *J. Biol. Chem.* **276:**43343–43350; 2001.

[36] Cai, D.; Leem, J. Y.; Greenfield, J. P.; Wang, P.; Kim, B. S.; Wang, R.; Lopes, K. O.; Kim, S. H.; Zheng, H.; Greengard, P.; Sisodia, S. S.; Thinakaran, G.; Xu, H. Presenilin-1 Regulates Intracellular Trafficking and Cell Surface Delivery of β-Amyloid Precursor Protein. *J. Biol. Chem.* **278:**3446–3454; 2003.

[37] Buss, H.; Chan, T. P.; Sluis, K. B.; Domigan, N. M.; Winterbourn, C. C. Protein carbonyl measurement by a sensitive ELISA method. *Free Radic. Biol. Med.* **23:** 361–366; 1997.

[38] Winterbourn, C. C.; Buss, I. H. Protein carbonyl measurement by enzyme linked immunosorbent assay. *Methods Enzymol.* **300:**106–111; 1999.

[39] Liao, X.; Liu, J. M.; Du, L.; Tang, A.; Shang, Y.; Wang, S. Q.; Chen, L. Y.; Chen, Q. Nitric oxide signaling in stretch-induced apoptosis of neonatal rat cardiomyocytes. *FASEB J.* **20:**1883–1885; 2006.

[40] Gutteridge, J. M.; Halliwell, B. The measurement and mechanism of lipid peroxidation in biological systems. *Trends. Biochem. Sci.* **15:**129–134; 1990.

[41] Pérez, A.; Morelli, L.; Cresto, J. C.; Castaño, E. M. Degradation of soluble amyloid β-peptides 1-40, 1-42, and the Dutch variant 1-40Q by insulin degrading enzyme from Alzheimer's disease and control brains. *Neurochem. Res.* **25:**247–255; 2000.

[42] Takeda, K.; Araki, W.; Tabira, T. Enhanced generation of intracellular Aβ42 amyloid peptide by mutation of presenilins PS1 and PS2. *Eur. J. Neurosci.* **19:**258–364; 2006.

[43] Smith, M. A.; Perry, G.; Richey, P. L.; Sayre, L. M.; Anderson, V. E.; Beal, M. F.; Kowall, N. Oxidative damage in Alzheimer's. *Nature* **382** (6587)**:**120–121; 1996.

[44] Mohmmad Abdul, H.; Wenk, G. L.; Gramling, M.; Hauss-Wegrzyniak, B.; Butterfield, D. A. APP and PS-1 mutations induce brain oxidative stress independent of dietary cholesterol: implications for Alzheimer's disease. *Neurosci. Lett.* **368:**148–150; 2004.

[45] Green, K. N.; Smith, I. F.; Laferla, F. M. Role of calcium in the pathogenesis of Alzheimer's disease and transgenic models. *Subcell. Biochem.* **45:**507–521; 2004.

[46] Thibault, O.; Gant, J. C.; Landfield, P. W. Expansion of the calcium hypothesis of brain aging and Alzheimer's disease: minding the store. *Aging Cell.* **6:**307–317; 2007.

[47] Brzyska, M.; Elbaum, D. Dysregulation of calcium in Alzheimer's disease. *Acta Neurobiol. Exp.* **63:**171–183; 2003.

[48] Butterfield, D. A.; Reed, T.; Newman, S. F.; Sultana, R. Roles of amyloid β-peptide-associated oxidative stress and brain protein modifications in the pathogenesis of Alzheimer's disease and mild cognitive impairment. *Free Radic. Biol. Med.* **43:** 658–677; 2007.

[49] Savage, M. J.; Lin, Y. G.; Ciallella, J. R.; Flood, D. G.; Scott, R. W. Activation of c-Jun N-terminal kinase and p38 in an Alzheimer's disease model is associated with amyloid deposition. *J. Neurosci.* **22:**3376–3385; 2002.

[50] Dineley, K. T.; Westerman, M.; Bui, D.; Bell, K.; Ashe, K. H.; Sweatt, J. D. β-Amyloid activates the mitogen-activated protein kinase cascade via hippocampal 7 nicotinic acetylcholine receptors: in vitro and in vivo mechanisms related to Alzheimer's disease. *J. Neurosci.* **21:**4125–4133; 2001.

[51] Han, P.; Dou, F.; Li, F.; Zhang, X.; Zhang, Y. W.; Zheng, H.; Lipton, S. A.; Xu, H.; Liao, F. F. Suppression of cyclin-dependent kinase 5 activation by amyloid precursor protein: a novel excitoprotective mechanism involving modulation of tau phosphorylation. *J. Neurosci.* **25:**11542–11552; 2005.

[52] Selkoe, D. J. Alzheimer's disease: genes, proteins, and therapy. *Physiol. Rev.* **81:** 741–766; 2001.

[53] Hardy, J.; Selkoe, D. J. The Amyloid Hypothesis of Alzheimer's Disease: Progress and Problems on the Road to Therapeutics. *Science* **297:**353–356; 2002.

[54] Tomita, T.; Iwatsubo, T. γ-Secretase as a Therapeutic Target for Treatment of Alzheimer's Disease. *Curr. Pharm. Des.* **12:**661–670; 2006.

[55] Lundkvist, J.; Näslund, J. γ-Secretase: a complex target for Alzheimer's disease. *Curr. Opin. Pharmacol.* **7:**112–118; 2007.

[56] Milano, J.; McKay, J.; Dagenais, C.; Foster-Brown, L.; Pognan, F.; Gadient, R.; Jacobs, R. T.; Zacco, A.; Greenberg, B.; Ciaccio, P. J. Modulation of notch processing by γ-secretase inhibitors causes intestinal goblet cell metaplasia and induction of genes known to specify gut secretory lineage differentiation. *Toxicol. Sci.* **82:** 341–358; 2004.

[57] Wolfe, M. S.; Xia, W.; Ostaszewski, B. L.; Diehl, T. S.; Kimberly, W. T.; Selkoe, D. J. Two transmembrane aspartates in presenilin-1 required for presenilin endoproteolysis and gamma-secretase activity. *Nature* **398:**513–517; 1999.

[58] Nunomura, A.; Perry, G.; Aliev, G.; Hirai, K.; Takeda, A.; Balraj, E. K.; Jones, P. K.; Ghanbari, H.; Wataya, T.; Shimohama, S.; Chiba, S.; Atwood, C. S.; Petersen, R. B.; Smith, M. A. Oxidative damage is the earliest event in Alzheimer disease. *J. Neuropathol. Exp. Neurol.* **60** (8)**:**759–767; 2001.

[59] Catalano, S. M.; Dodson, E. C.; Henze, D. A.; Joyce, J. G.; Krafft, G. A.; Kinney, G. G. The role of amyloid-beta derived diffusible ligands (ADDLs) in Alzheimer's disease. *Curr. Top Med. Chem.* **6** (6)**:**597–608; 2006.

[60] Behl, C.; Davis, J. B.; Lesley, R.; Schubert, D. Hydrogen peroxide mediates amyloid β-protein toxicity. *Cell* **77:**817–827; 1994.

[61] Huang, X.; Atwood, C. S.; Hartshorn, M. A.; Multhaup, G.; Goldstein, L. E.; Scarpa, R. C.; Cuajungco, M. P.; Gray, D. N.; Lim, J.; Moir, R. D.; Tanzi, R. E.; Bush, A. I. The Aβ-peptide of Alzheimer's disease directly produces hydrogen peroxide through metal ion reduction. *Biochemistry* **38:**7609–7616; 1999.

[62] Hensley, K.; Carney, J. M.; Mattson, M. P.; Aksenova, M.; Harris, M.; Wu, J. F.; Floyd, R. A.; Butterfield, D. A. A model for beta-amyloid aggregation and neurotoxicity based on free radical generation by the peptide: relevance to Alzheimer disease. *Proc. Natl. Acad. Sci. U. S. A.* **91:**3270–3274; 1994.

[63] Murakami, K.; Irie, K.; Ohigashi, H.; Hara, H.; Nagao, M.; Shimizu, T.; Shirasawa, T. Formation and stabilization model of the 42-mer Abeta radical: implications for the long-lasting oxidative stress in Alzheimer's disease. *J. Am. Chem. Soc.* **127:** 15168–15174; 2005.

[64] Tong, Y.; Zhou, W.; Fung, V.; Christensen, M. A.; Qing, H.; Sun, H.; Sun, X.; Song, W. Oxidative stress potentiates BACE1 gene expression and Abeta generation. *Neural. Transm.* **112:**455–469; 2005.

[65] Tamagno, E.; Guglielmotto, M.; Aragno, M.; Borghi, R.; Autelli, R.; Giliberto, L.; Muraca, G.; Danni, O.; Zhu, X.; Smith, M. A.; Perry, G.; Jo, D. G.; Mattson, M. P.; Tabaton, M. Oxidative stress activates a positive feedback between the gamma- and beta-secretase cleavages of the beta-amyloid precursor protein. *J. Neurochem.* **104** (3)**:**683–695; 2008.

[66] Steiner, B.; Marques, C. A.; Leutz, S.; Romig, H.; Haass, C.; Muller, W. E. Elevated vulnerability to oxidative stress-induced cell death and activation of caspase-3 by the Swedish amyloid precursor protein mutation. *J. Neurosci. R.* **64:**183–192; 2001.

[67] Loo, D. T.; Copani, A.; Pike, C. J.; Whittemore, E. R.; Walencewicz, A. J.; Cotman, C. W. Apoptosis is induced by β-amyloid in cultured central nervous system neurons. *Proc. Natl. Acad. Sci. U. S. A.* **90:**7951–7955; 1993.

[68] Mattson, M. P. Apoptosis in neurodegenerative disorders. *Nat. Rev. Mol. Cell Biol.* **1:** 120–129; 2000.

[69] Zhu, X.; Raina, A. K.; Rottkamp, C. A.; Aliev, G.; Perry, G.; Boux, H.; Smith, M. A. Activation and redistribution of c-jun N-terminal kinase/stress activated protein kinase in degenerating neurons in Alzheimer's disease. *J. Neurochem.* **76:**435–441; 2001.

[70] Zhu, X.; Castellani, R. J.; Takeda, A.; Nunomura, A.; Atwood, C. S.; Perry, G.; Smith, M. A. Differential activation of neuronal ERK, JNK/SAPK and p38 in Alzheimer disease: the 'two hit' hypothesis. *Mech. Ageing Dev.* **123** (1)**:**39–46; 2001.

[71] Zhu, X.; Raina, A. K.; Perry, G.; Smith, M. A. Alzheimer's disease: the two-hit hypothesis. *Lancet Neurol.* **3** (4)**:**219–226; 2004.
[72] Hansson Petersen, C. A.; Alikhani, N.; Behbahani, H.; Wiehager, B.; Pavlov, P. F.; Alafuzoff, I.; Leinonen, V.; Ito, A.; Winblad, B.; Glaser, E.; Ankarcrona, M. The amyloid beta-peptide is imported into mitochondria via the TOM import machinery and localized to mitochondrial cristae. *Proc. Natl. Acad. Sci. U. S. A.* **105:**13145–13150; 2008.
[73] Saavedra, L.; Mohamed, A.; Ma, V.; Kar, S.; de Chaves, E. P. Internalization of beta amyloid peptide by primary neurons in the absence of apolipoprotein E. *J. Biol. Chem.* **282:**35722–35732; 2007.
[74] Ma, Q. L.; Lim, G. P.; Harris-White, M. E.; Yang, F.; Ambegaokar, S. S.; Ubeda, O. J.; Glabe, C. G.; Teter, B.; Frautschy, S. A.; Cole, G. M. Antibodies against beta-amyloid reduce Abeta oligomers, glycogen synthase kinase-3beta activation and tau phosphorylation in vivo and in vitro. *J. Neurosci. Res.* **83** (3)**:**374–384; 2006.